ACS APPLIED MATERIALS & INTERFACES

Research Article

Cite This: ACS Appl. Mater. Interfaces 2019, 11, 46212−46218

www.acsami.org

Rapid, Localized, and Athermal Shape Memory Performance Triggered by Photoswitchable Glass Transition Temperature

Xiao Zhang, Chongyu Zhu, Bo Xu, Lang Qin, Jia Wei, and Yanlei Yu*

Department of Materials Science and State Key Laboratory of Molecular Engineering of Polymers, Fudan University, 220 Handan Road, Shanghai, 200433, China

Supporting Information

ABSTRACT: Shape memory polymers that undergo shape recovery at room temperature (RT) are desirable for their potential in vivo applications, yet challenging. Herein, light-triggered athermal shape memory effect of azopolymer networks is reported by photoswitching the glass transition temperature (T_g) rather than external heating. Thanks to the switchable T_g of azopolymer induced by reversible *trans*−*cis* isomerization, the entropic energy is trapped in low T_g state (*cis*-form T_g < RT) to deform into a temporary shape and fixed in high T_g state (*trans*-form T_g > RT). Upon exposure to UV light, the reduced low T_g allows release of the entropic energy, realizing athermal shape recovery of the permanent shape. By exploring the shape memory performance, we demonstrate diverse light-induced rapid shape recovery from temporary shape to original shape. Because of the instant, precise, and spatiotemporal manipulation of light, programmable shape recovery of surface topography is further extended. We anticipate that this strategy will provide tremendous opportunities for future precise medicine devices and soft robotics.

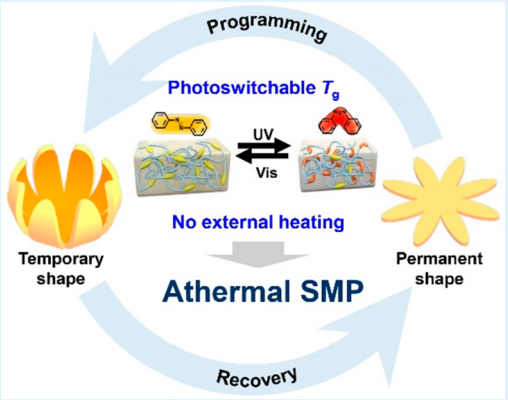

KEYWORDS: *athermal shape memory effect, azopolymer, switchable glass transition temperature, rapid activation, photoresponse*

INTRODUCTION

Shape memory polymers (SMPs) are burgeoning intelligent materials capable of memorizing a predefined temporary shape and reverting to their original shape when triggered by external stimuli, allowing diverse applications in the fields of biomedicine,[1−7] aerospace,[8−10] flexible electronics,[11−13] and nanofabrication.[14−17] Although various forms of external stimuli are employed to trigger shape memory, the most extensively investigated one is heating.[18−22] Upon heating of these materials above the glass transition temperature (T_g), the chain mobility is significantly activated to change conformation under external stress, leading to a temporary shape with low entropy, which is fixed by subsequent cooling. The shape recovery occurs when the polymer is reheated to release the stored entropic energy, revealing the shape memory effect.[23−25] Although direct heating or inductive heating is most commonly employed to trigger shape recovery,[26−29] the access to heating is not feasible for in vivo operations.[7] Alternative external stimuli (e.g., moisture, magnetic field, and chemical solvent) have been utilized to activate shape recovery but still suffer from the long activation time and imprecise manipulation.[30−35] Light is considered as an attractive stimulus on account of its capability for temporal, localized, remote, and isothermal triggering and actuation.[36−40] Thus, light-induced SMPs that undergo shape recovery at room temperature (RT), that is, athermal SMPs (ASMPs), are desirable in microscale operation under actual working conditions.

Generally, the entropic energy is the driving force for shape memory behavior in polymeric systems that is generated by the chain conformational change during macroscale deformation. Lendlein developed an innovative strategy to realize light-activated shape memory based on reversible cinnamate chemistry, for which the shape fixing and recovery were enabled by changing the cross-link density of the network.[41] The entropic energy arising from external force was stored and released by the reconfiguration and breaking of chemical bonds, resulting in the macroscopic shape memory effect. However, this instance was still limited by the low shape fixity because of the elastic contraction of the stretched chain segments and long activation time due to slow photochemical reaction in bulk. Therefore, light-induced ASMPs with rapid activation speed and high shape memory functionality are alluring but remain a great challenge and opportunity.

Herein, we report a strategy to trigger athermal shape memory effect rapidly in an azobenzene-containing polymer network (APN) by photoswitching the T_g. Upon sequential ultraviolet (UV) and visible-light illumination, the T_g of APN is switched below or above RT, triggering the athermal shape memory effect. Remarkable, various rapid shape recoveries of the APN actuators are realized to explore the shape memory performance.

Received: September 23, 2019
Accepted: November 13, 2019
Published: November 13, 2019

DOI: 10.1021/acsami.9b17271
ACS Appl. Mater. Interfaces 2019, 11, 46212−46218

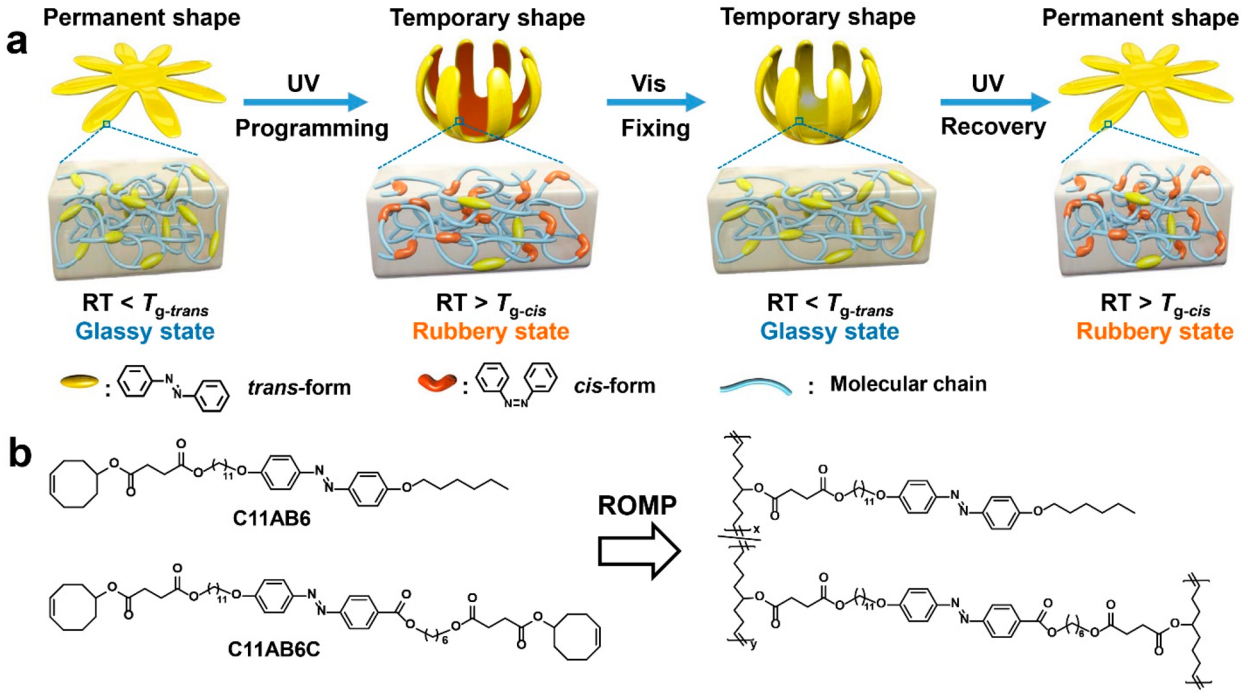

Figure 1. Athermal shape memory effect and synthesis of the APN. (a) Shape memory effect of a modeling flower and the mechanism of athermal shape memory effect. The azobenzene units in their permanent shape are in the *trans* form and the $T_{g\text{-}trans}$ of APN is above RT. After UV irradiation, the *trans*-form APN isomerizes to *cis* form, whose $T_{g\text{-}cis}$ is below RT, and the permanent shape is thus programmed to a temporary shape under external stress. The temporary shape is then fixed by the following visible-light illumination, in which the $T_{g\text{-}trans}$ of APN is above RT. At last, the temporary shape reverts to its permanent shape when exposed to UV light again. (b) Synthesis of the APN via ring-opening metathesis polymerization (ROMP).

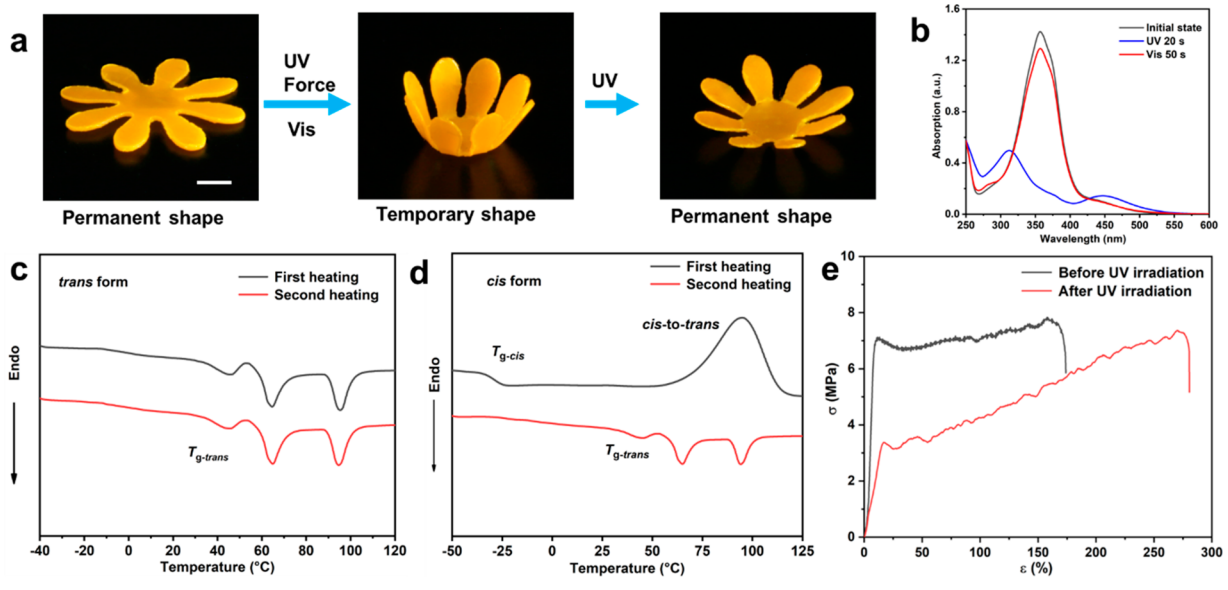

Figure 2. Light-induced shape memory performance and the characterization of T_g before and after UV irradiation. (a) Athermal shape memory effect of a cosmos sample. (b) UV−vis absorption spectra of the APN film before irradiation, after UV irradiation (365 nm, 40 mW cm^{-2}, 20 s), and subsequent visible-light irradiation (530 nm, 30 mW cm^{-2}, 50 s). (c) DSC curves of the *trans*-form APN sample. The *trans*-form APN sample shows a glass transition temperature at 42 °C and two phase transition temperatures at 70 and 95 °C in both heating curves. (d) DSC curves of the *cis*-form APN sample. The second heating DSC curve of this sample is the same as that of the *trans*-form APN sample, showing that the *cis* form is thermally converted to the *trans* form in the first heating process. (e) Stress−strain curves of the APN strip before (black line) and after UV irradiation (red line). The elasticity modulus of the APN strip before UV irradiation is about 130 MPa and the elongation at break reaches 160%. After UV irradiation for 1 min, the elasticity modulus reduces 23 MPa and the elongation at break increases to 280%.

Thanks to the remote and localized control of light, we demonstrate the programmable shape recovery of digital number upon partial UV irradiation, providing potential applications for future precise medicine and intelligent devices.

RESULTS AND DISCUSSION

The prerequisite of our strategy is switching the intrinsic T_g of APN. Recently, azopolymers have been verified to possess switchable T_g via photoisomerization of azobenzene, resulting in

DOI: 10.1021/acsami.9b17271
ACS Appl. Mater. Interfaces 2019, 11, 46212−46218

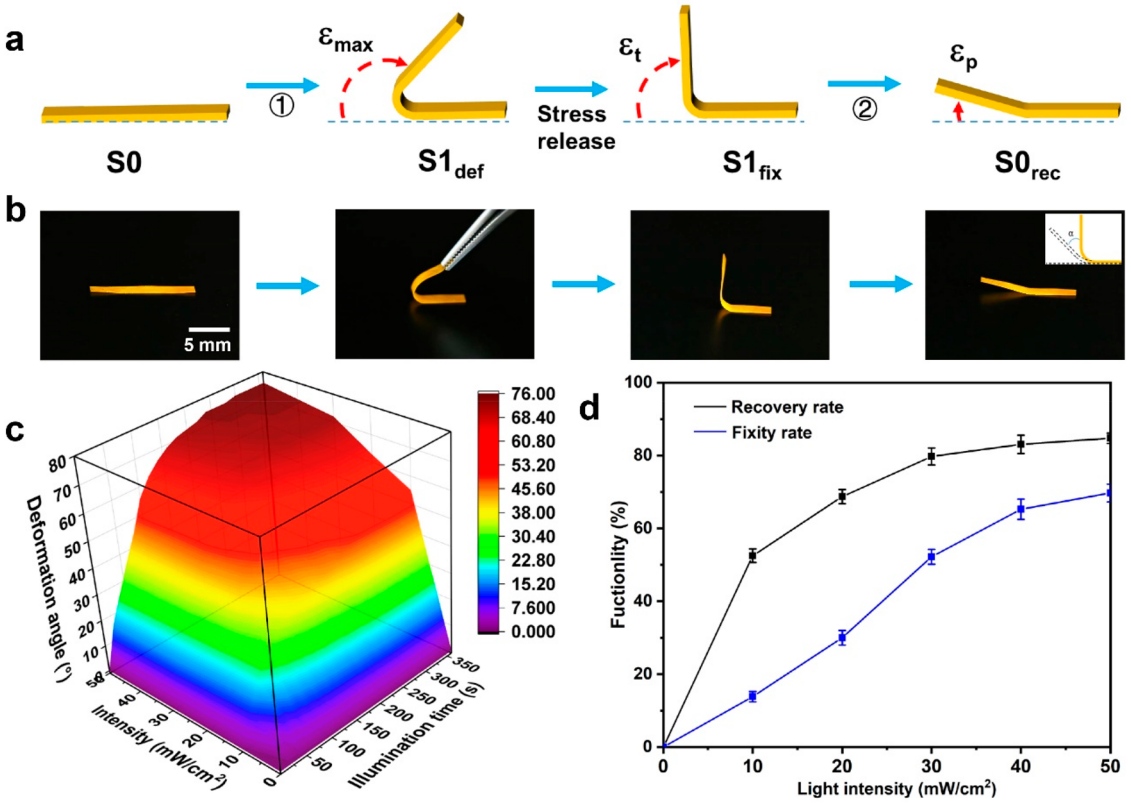

Figure 3. Shape recovery under various light intensities. (a) Programming and recovery protocols of light-induced shape memory performance. The aligned blue dashed line records the position of permanent shape (straight rod). (b) Images of the strip sample (10 mm × 1 mm × 0.05 mm) at different stages during programming and the corresponding shape recovery process. (c) Influence of light intensity on the shape memory behavior of the APN strip. (d) Fixity rate and the recovery rate of the APN strip upon exposure to UV light with different intensities.

reversible transition between glassy state (*trans* form, low chain mobility) and rubbery state (*cis* form, high chain mobility).[42,43] Following this theory, we propose an original method for light-activated athermal shape memory effect of the APN. The key strategy is to store and release entropic energy by utilizing the reversible transition, which is the driving force for the shape recovery. The detailed process of programming and recovery are schematized in Figure 1a. First, the modeling APN is processed into a permanent blooming sunflower shape, whose $T_{g\text{-}trans}$ is above RT. Then the permanent shape is irradiated with UV light (365 nm) and the *trans*-form azobenzene units isomerize to the *cis* form, resulting in the $T_{g\text{-}cis}$ of APN below RT. Therefore, the permanent shape is ready to be programmed into a temporary shape under external stress. Next, the temporary shape is fixed after the subsequent illumination of visible light (530 nm) to conduct *cis*−*trans* isomerization ($T_{g\text{-}trans}$ is above RT). Shape recovery of the permanent shape is triggered by the irradiation of UV light, reducing the $T_{g\text{-}cis}$ below RT to release the stored entropic energy. Compared to traditional thermo-induced SMPs, the shape programming and recovery of the APN are performed at RT without auxiliary heating, revealing the athermal shape memory effect.

To satisfy the criterions that SMPs are polymer networks equipped with suitable stimuli-sensitive molecular switches, we chose the chemical cross-linked APN as a model network to illustrate the athermal shape memory effect under RT. The rationally designed APN was synthesized with the cyclooctene monomer C11AB6 and cross-linker C11AB6C by ring-opening metathesis polymerization (Figure 1b). The photoresponsive azobenzene units of the APN act as the switch segments and the cross-linked points are responsible for linking the segments and determining the permanent shape. The long spacers provide enough free volume for the azobenzene units to undergo a fast photoisomerization.

Shapes of thermoset SMPs are permanently defined three-dimensionally (3D) by the interconnected network of covalent bonds which are typically robust but irreversible, making them unmalleable. To overcome the processing bottleneck, we incorporated dynamic ester bonds to endow the thermoset cross-linked APN with reshaping, allowing infinite design of permanent shapes.[44−46] The catalytic transesterification reaction was activated at high temperature and allowed for rearrangement of polymer chain in the matrix, thus affording plasticity and easy processability. Taking advantage of malleable networks, we prepared various 2D and 3D permanent shapes in different molds at 180 °C for 3 h (Figure S3, Supporting Information).

Specifically, a cosmos sample was fabricated to illustrate the light-induced athermal shape memory behavior at RT (Figure 2a). We first prepared an artificial cosmos in the open state, and then the cosmos was forced to the closed state after UV illumination and fixed by visible-light irradiation. The closed cosmos recovered its original open state upon exposure to UV light subsequently, exhibiting the athermal shape memory effect (Movie S1).

The photoisomerization of azobenzene was characterized by UV−vis absorption spectroscopy (Figure 2b). Irradiating the APN film in the initial state with 365 nm UV light decreased the intensities of the π−π*band ($\lambda \approx 356$ nm) of the *trans* isomer, resulting in a high *trans*−*cis* isomerization efficiency of 87%,

DOI: 10.1021/acsami.9b17271
ACS Appl. Mater. Interfaces 2019, 11, 46212−46218

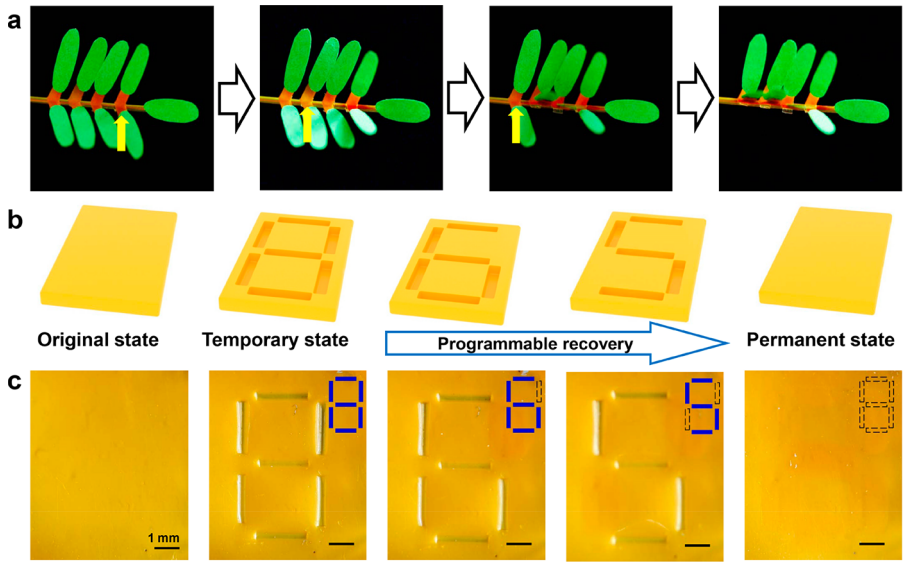

Figure 4. Localized and programmable shape recovery. (a) Stimuli-response behavior of artificial mimosa. Programmable shape recovery of artificial mimosa with step-by-step stimuli of UV illumination. The leaves of the mimosa were tailored with commercial green paper and the pulvinus was fabricated with the shape memory APN. The yellow arrow represents the illumination position of UV light. (b) Schematic illustration of programmable shape memory performance of surface digital number. (c) Programmable recovery of surface topography. A sunken pattern "8" is temporarily constructed on a flat APN surface. After illumination of localized UV light (365 nm, 40 mW cm^{-2}) and visible light (530 nm, 50 mW cm^{-2}), the sunken number "8" converts into the new number "6" and number "5". Finally, the number "5" reverts back to the original flat state.

while irradiating with 530 nm light led to a *cis*−*trans* isomerization efficiency of 83%. To further understand the mechanism of athermal shape memory effect, we analyzed the T_g of APN before and after UV irradiation using differential scanning calorimetry (DSC). The *trans*-form APN performed glass transition at 42 °C in the heating curves (Figure 2c), indicating that the chain segments were frozen at RT in trans form. Next, the *cis*-form APN was obtained by irradiating the *trans*-form APN with UV irradiation (Figure S4). In contrast to the *trans*-form APN, the *cis* form showed an extremely low T_g at −28 °C (far below RT) and a broad exothermic band at 80∼120 °C induced by thermal *cis*−*trans* isomerization (Figure 2d). The reduction of T_g is attributed to the stacking and orientation change induced by *trans*−*cis* photoisomerization of azobenzene units.[42] Thus, the molecular chains in the *cis* form are active to store entropic energy at RT. The second heating DSC curve of the *cis*-form APN was identical to that of the *trans*-form APN because of the thermal conversion to the *trans* form in the first heating process. Owing to the switchable T_g caused by *trans* to *cis* isomerization of azobenzene, the chain segments of the APN are selectively activated or frozen at RT, which is employed to store and release the entropic energy. Therefore, the athermal shape memory effect was achieved by adjusting its T_g between 42 and −28 °C upon different light irradiation.

Furthermore, the variation on mechanical properties of the APN before and after UV irradiation were tested to verify the difference of the T_g. As shown in Figure 2e, the elasticity modulus of the APN strip before UV irradiation is about 130 MPa and the elongation at break reaches 160%. After UV irradiation for 1 min, the APN strip isomerized from *trans* to *cis* form with the T_g below room temperature. The elasticity modulus reduces to 23 MPa and the elongation at break increases to 280%, which indicates that the APN strip switches from glassy state to rubbery state after UV irradiation.

The light intensity is the key parameter impacting the shape memory behavior. Aiming to explore a rational light intensity, we systematically studied via photomechanical experiments the shape memory behaviors with different light intensities (Figure 3a). As the intensity of UV light increases from 10 to 50 mW cm^{-2}, the recovery angle α (defined in Figure 3b) of the APN strip enlarges from 45° to 76° (Figure 3c), exhibiting the highest final shape recovery ratio of 85%, and the fixity ratio of the APN strip increases from 16% to 70% (Figure 3d). We noted that the weak UV light leads to a low recovery angle; a plausible reason was the visible light in the natural light counteracting the *trans*−*cis* isomerization. This deterioration was progressively remitted with the increasing intensity of UV light. Besides, the reduction in shape recovery time of film with a stronger light intensity was attributed to the high efficiency of *trans*−*cis* isomerization (87%), leading to rapid shape recovery. Compared to a previous report of light-activated SMP systems with long activation time of 1 h, our shape memory strategy exhibited much faster actuation in 60 s.[41] Moreover, the photothermal effect in the shape memory process was evaluated by infrared thermal imaging method. The maximum temperature increased from 18.4 to 19.6 °C (Figure S5), which was far below the $T_{g\text{-}trans}$ of APN, indicating that the shape recovery was triggered by intrinsic T_g switching rather than photothermal effect. Taking the aforementioned into consideration, 40 mW cm^{-2} is selected for the remaining experiments to observe shape recovery on a feasible time scale and ensure that no significant heat was generated upon illumination.

Localized and programmable shape recovery is further extended by taking advantage of the precise, spatiotemporal control of light. Mimosas are typical sensitive plants that are capable of response to adventitious stimulus, closing their leaves to protect themselves. Inspired by the rapid leaf movement of mimosa, artificial mimosa was manufactured with the shape memory APN, commercial green paper, and plastic stick. The APN in the artificial mimosa acts as the responsive section similar to the motor cells in the natural mimosa. After irradiation with 365 nm light, the closed leaves were deformed into the

DOI: 10.1021/acsami.9b17271
ACS Appl. Mater. Interfaces 2019, 11, 46212−46218

open state by applying external force and fixed by 530 nm light. As shown in Figure 4a, the leaves of mimosa underwent rapid shape recovery from open to closed state individually with the movement of UV light, exhibiting fast response characteristic that is similar to the stimuli-responsive process of natural mimosa (Movie S2). Different from the typical thermo-induced SMPs whose overall recovery occurred upon heating above the transition temperature, the athermal and precise control of light also offers a way for programmable shape memory behavior, which is suitable for the construction of digital information. A sunken digital number "8" was temporarily constructed on a flat APN surface. Afterward, the digital number "8" was partially irradiated with UV light to trigger the shape recovery of the exposed area, programming a new digital number "6". Similarly, another digital number "5" is displayed after subsequent localized irradiation of UV light. The digital number "5" recovered to the original flat state eventually when the whole area was exposed to UV light, revealing programmable shape recovery of light-induced ASMP (Figure 4c). The programmable recovery of light-induced ASMP is easily integrated into applications of anticounterfeiting and encryption.

Despite the unique features of isothermal and programmable triggering, the actuation of ASMP sample is not limited to an unloaded state. We prepared a sample with a permanent arched shape, and it was programmed to a temporary flat shape. During the recovery from flat shape to arched shape, the sample lifted a load 50 times heavier than the weight of the actuator because of the geometry difference (Figure S7 and Movie S4). This characteristic is particular useful in biomedicine in which both athermal effect and loaded actuation are critical for in situ manipulation.

CONCLUSIONS

In summary, we have developed a strategy to realize the athermal shape memory effect by photoswitching the T_g of APN. The cross-linked APN is readily reshaped into thin films and diverse 3D structures on heating by rearrangement of network topology due to transesterification of dynamic ester bonds. Thanks to the switchable T_g of APN induced by reversible *trans*−*cis* isomerization of azobenzene groups, the entropic energy is stored and released via the switching between rubbery state and glassy state upon illumination. Therefore, we successfully demonstrate the athermal shape memory behavior of cosmos sample at RT without external heating. Because of the high spatiotemporal resolution to precisely manipulate light, we also demonstrate the programmable shape recovery of digital number with 365 nm light. This work sets up a moderate and effective strategy to trigger shape memory effect at RT by remote activation, which eliminates the temperature constraints of thermoresponsive shape memory polymers. We anticipate that the unique athermal shape memory effect will provide tremendous opportunities for future precise medicine, soft robotics, and automation equipment.

EXPERIMENTAL SECTION

Materials. 1-(3-(Dimethylamino)propyl)-3-ethylcarbodiimide hydrochloride (EDC) was obtained from Adamas. Dimethylaminopyridine (DMAP), dimethylaminopyridine (DMF), and dichloromethane (CH_2Cl_2) were obtained from Taitan Technologies. Grubb's Second Generation catalyst and 1,5,7-triazabicyclo [4.4.0] dec-5-ene (TBD) were purchased from Sigma-Aldrich. All chemicals were purchased commercially and used as-received.

Synthesis of the APN Network. Synthesis of azobenzene derivative is described in the Supporting Information (Figure S1). Typically, $C_{11}AB_6$ (475 mg, 95 wt %) and $C_{11}AB_6C$ (25 mg, 5 wt %) were placed into a Schlenk flask. The anhydrous CH_2Cl_2 solution (1.5 mL) of Grubb's Second Generation catalyst (0.5 mg) was injected into a flask via syringe under argon. The resulting mixture was stirred at 50 °C for 4 h to yield orange-yellow polymer. The polymer was further dried in an oven for 1 h. Then the polymer bulk and [1,5,7-triazabicyclo[4.4.0]dec-5-ene (TBD)] (3 wt %) were added to the CH_2Cl_2 (10 mL) and stood for 6 h to obtain a swollen polymer. The swollen polymer was vacuum-dried at 50 °C overnight to gain the APN bulk.

Preparation of the APN Films and Actuators. The thin films were prepared by hot-pressing the polymer solid at 130 °C, followed by cooling to room temperature. The films were pretailored into 2D shapes, which were then folded and fixed by a mold with a temperature above 130 °C for 3 h, obtaining the 3D samples by cooling to room temperature. Other 3D samples were fabricated by the same method with different molds. The APN pattern was obtained by pressing the film between a flat glass substrate and a template. Peeling off the template from the polymer film created the digital pattern.

Shape Memory Functionality. The light-induced shape memory functionality of the polymers was quantified by photomechanical experiments at room temperature. Initially, the sample was exposed to UV light and bent to ε_{max}. Upon illumination of visible light for 3 min and releasing of the stress, a temporary shape with a bending angle of ε_t was observed. The temporary bending strip reverted to its permanent shape with remaining bending angle ε_p. The experiment allowed the calculation of the fixity rate and recovery rate through the equation $R_f = \varepsilon_t/\varepsilon_{max}$ and $R_r = (\varepsilon_t - \varepsilon_p)/\varepsilon_t$.

Photoisomerization Efficiency. The isomerization efficiency is calculated to be 87% from the UV−vis absorption spectra using the method described in the literature.[47,48] The equation to obtain the isomerization efficiency is shown below: $\eta = (A_0 - A_{eq})/A_0 \times 100\%$ (A_{eq} is the absorptivity in the photostationary state and A_0 is the absorptivity in the original state).

Characterization. The thermodynamic properties of the *trans-/cis*-form azopolymers determined by differential scanning calorimetry (DSC) experiments were carried out under a nitrogen atmosphere on TA Instruments DSC Q2000 at a heating rate and cooling rate of 20 °C/min. UV−vis absorption spectra were recorded on a PerkinElmer Lambda 650 spectrometer. ^{1}H NMR spectra of the monomers were recorded on a Bruker DMX500 NMR spectrometer using tetramethylsilane (TMS) as the internal standard and $CDCl_3$ as solvent. UV light (365 nm) was generated by an Omron ZUV-H30MC light source with a ZUV-C30H controller; green light (530 nm) was generated by a CCS HLV-24GR-3W light source with a PJ-1505-2CA controller. Photographs and videos of the deformation behaviors as well as the light-induced liquid motion were taken by a commercial cannon camera (70D). The temperature of irradiating SMP sample was obtained by the FLIR E40 infrared imager.

ASSOCIATED CONTENT

Supporting Information

The Supporting Information is available free of charge at https://pubs.acs.org/doi/10.1021/acsami.9b17271.

Movie 1: Shape recovery of the cosmos flower: from a closed state to an open state; when the temporary closed flower is placed under a UV light, the cosmos flower recovers to the initial state during illumination (MP4)

Movie 2: Localized shape recovery of the artificial mimosa induced by the UV light spot; leaves of the mimosa underwent rapid shape recovery from an open state to a closed state individually with the movement of the UV light (MP4)

Movie 3: Programmable shape recovery of the zigzag strip; zigzag strip stepwise recovered to a straight strip by programmed illumination of UV light (MP4)

DOI: 10.1021/acsami.9b17271
ACS Appl. Mater. Interfaces 2019, 11, 46212−46218

Movie 4: Shape recovery of the APN sample in the presence of a load; during the recovery from a flat shape to an arched shape, the sample lifted up a load 50 times heavier than the weight of the actuator because of the geometry difference (MP4)

Experimental section, characterization of materials, and additional demonstrations of the APN actuators (PDF)

AUTHOR INFORMATION

Corresponding Author

*E-mail: ylyu@fudan.edu.cn (Y.L.Y.).

ORCID

Yanlei Yu: 0000-0002-4623-3331

Author Contributions

Y.L.Y. conceived the idea and led the project; X.Z., B.X., L.Q., J.W., and Y.L.Y. designed the experiments; X.Z. and B.X. performed the experiments; X.Z., L.Q., and J.W. analyzed the experimental data. X.Z., C.Y.Z., L.Q., and Y.L.Y. wrote the paper.

Notes

The authors declare no competing financial interest.

ACKNOWLEDGMENTS

This work was supported financially from the National Natural Science Foundation of China (21734003), the National Key R&D Program of China (2016YFA0202902), and Innovation Program of Shanghai Municipal Education Commission (2017-01-07-00-07-E00027)

REFERENCES

(1) Lendlein, A.; Langer, R. Biodegradable, Elastic Shape-Memory Polymers for Potential Biomedical Applications. *Science* **2002**, *296*, 1673−1676.

(2) Hardy, J. G.; Palma, M.; Wind, S. J.; Biggs, M. J. Responsive Biomaterials: Advances in Materials Based on Shape-Memory Polymers. *Adv. Mater.* **2016**, *28*, 5717−5724.

(3) Neffe, A. T.; Hanh, B. D.; Steuer, S.; Lendlein, A. Polymer Networks Combining Controlled Drug Release, Biodegradation, and Shape Memory Capability. *Adv. Mater.* **2009**, *21*, 3394−3398.

(4) Kratz, K.; Voigt, U.; Lendlein, A. Temperature-Memory Effect of Copolyesterurethanes and Their Application Potential in Minimally Invasive Medical Technologies. *Adv. Funct. Mater.* **2012**, *22*, 3057−3065.

(5) Wei, H. Q.; Zhang, Q. W.; Yao, Y. T.; Liu, L. W.; Liu, Y. J.; Leng, J. S. Direct-Write Fabrication of 4D Active Shape-Changing Structures Based on a Shape Memory Polymer and Its Nanocomposite. *ACS Appl. Mater. Interfaces* **2017**, *9*, 876−883.

(6) Landsman, T. L.; Touchet, T.; Hasan, S. M.; Smith, C.; Russell, B.; Rivera, J.; Maitland, D. J.; Cosgriff-Hernandez, E. A Shape Memory Foam Composite with Enhanced Fluid Uptake and Bactericidal Properties as A Hemostatic Agent. *Acta Biomater.* **2017**, *47*, 91−99.

(7) Small, W., IV; Singhal, P.; Wilson, T. S.; Maitland, D. J. Biomedical Applications of Thermally Activated Shape Memory Polymers. *J. Mater. Chem.* **2010**, *20*, 3356−3366.

(8) Liu, Y. J.; Du, H. Y.; Liu, L. W.; Leng, J. S. Shape Memory Polymers and Their Composites in Aerospace Applications: A Review. *Smart Mater. Struct.* **2014**, *23*, 023001.

(9) Cho, J. W.; Kim, J. W.; Jung, Y. C.; Goo, N. S. Electroactive Shape-Memory Polyurethane Composites Incorporating Carbon Nanotubes. *Macromol. Rapid Commun.* **2005**, *26*, 412−416.

(10) Leng, J. S.; Lan, X.; Liu, Y. J.; Du, S. Y.; Huang, W. M.; Liu, N.; Phee, S. J.; Yuan, Q. Electrical Conductivity of Thermoresponsive Shape-Memory Polymer with Embedded Micron Sized Ni Powder Chains. *Appl. Phys. Lett.* **2008**, *92*, 014104.

(11) Huang, Y.; Zheng, N.; Cheng, Z.; Chen, Y.; Lu, B.; Xie, T.; Feng, X. Direct Laser Writing-Based Programmable Transfer Printing via Bioinspired Shape Memory Reversible Adhesive. *ACS Appl. Mater. Interfaces* **2016**, *8*, 35628−35633.

(12) Wang, X. J.; Guo, X. G.; Ye, J. L.; Zheng, N.; Kohli, P.; Choi, D.; Zhang, Y.; Xie, Z. Q.; Zhang, Q. H.; Luan, H. W.; Nan, K. W.; Kim, B. H.; Xu, Y. M.; Shan, X. W.; Bai, W. B.; Sun, R. J.; Wang, Z. Z.; Jang, H. Y.; Zhang, F.; Ma, Y. J.; Xu, Z.; Feng, X.; Xie, T.; Huang, Y. G.; Zhang, Y. H.; Rogers, J. A. Freestanding 3D Mesostructures, Functional Devices, and Shape-Programmable Systems Based on Mechanically Induced Assembly with Shape Memory Polymers. *Adv. Mater.* **2019**, *31*, 1805615.

(13) Zarek, M.; Layani, M.; Cooperstein, I.; Sachyani, E.; Cohn, D.; Magdassi, S. 3D Printing of Shape Memory Polymers for Flexible Electronic Devices. *Adv. Mater.* **2016**, *28*, 4449−4454.

(14) Lee, E.; Zhang, M.; Cho, Y.; Cui, Y.; Van der Spiegel, J.; Engheta, N.; Yang, S. Tilted Pillars on Wrinkled Elastomers as A Reversibly Tunable Optical Window. *Adv. Mater.* **2014**, *26*, 4127−4133.

(15) Chen, C. M.; Chiang, C. L.; Lai, C. L.; Xie, T.; Yang, S. Buckling-Based Strong Dry Adhesives via Interlocking. *Adv. Funct. Mater.* **2013**, *23*, 3813−3823.

(16) Chen, C. M.; Yang, S. Directed Water Shedding on High-Aspect-Ratio Shape Memory Polymer Micropillar Arrays. *Adv. Mater.* **2014**, *26*, 1283−1288.

(17) Xu, H.; Yu, C.; Wang, S.; Malyarchuk, V.; Xie, T.; Rogers, J. A. Deformable, Programmable, and Shape-Memorizing Micro-Optics. *Adv. Funct. Mater.* **2013**, *23*, 3299−3306.

(18) Xie, T. Tunable Polymer Multi-Shape Memory Effect. *Nature* **2010**, *464*, 267−270.

(19) Mohr, R.; Kratz, K.; Weigel, T.; Lucka-Gabor, M.; Moneke, M.; Lendlein, A. Initiation of Shape-Memory Effect by Inductive Heating of Magnetic Nanoparticles in Thermoplastic Polymers. *Proc. Natl. Acad. Sci. U. S. A.* **2006**, *103*, 3540−3545.

(20) Tippets, C. A.; Li, Q.; Fu, Y.; Donev, E. U.; Zhou, J.; Turner, S. A.; Jackson, A.M. S.; Ashby, V. S.; Sheiko, S. S.; Lopez, R. Dynamic Optical Gratings Accessed by Reversible Shape Memory. *ACS Appl. Mater. Interfaces* **2015**, *7*, 14288−14293.

(21) Razzaq, M. Y.; Behl, M.; Lendlein, A. Magnetic Memory Effect of Nanocomposites. *Adv. Funct. Mater.* **2012**, *22*, 184−191.

(22) Habault, D.; Zhang, H.; Zhao, Y. Light-Triggered Self-Healing and Shape-Memory Polymers. *Chem. Soc. Rev.* **2013**, *42*, 7244−7256.

(23) Lendlein, A.; Gould, O. E. C. Reprogrammable Recovery and Actuation Behaviour of Shape-Memory Polymers. *Nat. Rev. Mater.* **2019**, *4*, 116−133.

(24) Behl, M.; Razzaq, M. Y.; Lendlein, A. Multifunctional Shape-Memory Polymers. *Adv. Mater.* **2010**, *22*, 3388−3410.

(25) Xie, T. Recent Advances in Polymer Shape Memory. *Polymer* **2011**, *52*, 4985−5000.

(26) McBride, M. K.; Martinez, A. M.; Cox, L.; Alim, M.; Childress, K.; Beiswinger, M.; Podgorski, M.; Worrell, B. T.; Killgore, J.; Bowman, C. N. A Readily Programmable, Fully Reversible Shape-Switching Material. *Sci. Adv.* **2018**, *4*, No. eaat4634.

(27) Miao, S.; Cui, H.; Nowicki, M.; Xia, L.; Zhou, X.; Lee, S.-J.; Zhu, W.; Sarkar, K.; Zhang, Z.; Zhang, L. G. Stereolithographic 4D Bioprinting of Multiresponsive Architectures for Neural Engineering. *Adv. Bio.* **2018**, *2*, 1800101.

(28) van Manen, T.; Janbaz, S.; Zadpoor, A. A. Programming the Shape-Shifting of Flat Soft Matter. *Mater. Today* **2018**, *21*, 144−163.

(29) Yang, H.; Leow, W. R.; Wang, T.; Wang, J.; Yu, J. C.; He, K.; Qi, D. P.; Wan, C. J.; Chen, X. D. 3D Printed Photoresponsive Devices Based on Shape Memory Composites. *Adv. Mater.* **2017**, *29*, 1701627.

(30) Huang, W. M.; Yang, B.; An, L.; Li, C.; Chan, Y. S. Water-Driven Programmable Polyurethane Shape Memory Polymer: Demonstration and Mechanism. *Appl. Phys. Lett.* **2005**, *86*, 114105.

(31) He, Z. W.; Satarkar, N.; Xie, T.; Cheng, Y. T.; Hilt, J. Z. Remote Controlled Multishape Polymer Nanocomposites with Selective Radiofrequency Actuations. *Adv. Mater.* **2011**, *23*, 3192−3196.

(32) Xiao, R.; Nguyen, T. D. Modeling The Solvent-Induced Shape-Memory Behavior of Glassy Polymers. *Soft Matter* **2013**, *9*, 9455−9464.

DOI: 10.1021/acsami.9b17271
ACS Appl. Mater. Interfaces 2019, 11, 46212−46218

(33) Xiao, R.; Guo, J.; Safranski, D.; Nguyen, T. D. Solvent-Driven Temperature Memory and Multiple Shape Memory Effects. *Soft Matter* **2015**, *11*, 3977−3985.
(34) Wang, C.; Fadeev, M.; Zhang, J. J.; Vazquez-Gonzalez, M.; Davidson-Rozenfeld, G.; Tian, H.; Willner, I. Shape-Memory and Self-Healing Functions of DNA-Based Carboxymethyl Cellulose Hydrogels Driven by Chemical or Light Triggers. *Chem. Sci.* **2018**, *9*, 7145−7152.
(35) Li, Z. Y.; Davidson-Rozenfeld, G.; Vazquez-Gonzalez, M.; Fadeev, M.; Zhang, J. J.; Tian, H.; Willner, I. Multi-triggered Supramolecular DNA/Bipyridinium Dithienylethene Hydrogels Driven by Light, Redox, and Chemical Stimuli for Shape-Memory and Self-Healing Applications. *J. Am. Chem. Soc.* **2018**, *140*, 17691−17701.
(36) Qin, L.; Gu, W.; Wei, J.; Yu, Y. L. Piecewise Phototuning of Self-Organized Helical Superstructures. *Adv. Mater.* **2018**, *30*, 1704941.
(37) Lv, J. A.; Liu, Y. Y.; Wei, J.; Chen, E. Q.; Qin, L.; Yu, Y. L. Photocontrol of Fluid Slugs in Liquid Crystal Polymer Microactuators. *Nature* **2016**, *537*, 179−184.
(38) Qian, X.; Chen, Q.; Yang, Y.; Xu, Y.; Li, Z.; Wang, Z.; Wu, Y.; Wei, Y.; Ji, Y. Untethered Recyclable Tubular Actuators with Versatile Locomotion for Soft Continuum Robots. *Adv. Mater.* **2018**, *30*, 1801103.
(39) Wei, J.; Yu, Y. L. Photodeformable Polymer Gels and Crosslinked Liquid-Crystalline Polymers. *Soft Matter* **2012**, *8*, 8050−8059.
(40) Lu, X. L.; Guo, S. W.; Tong, X.; Xia, H. S.; Zhao, Y. Tunable Photocontrolled Motions Using Stored StrainEnergy in Malleable Azobenzene Liquid Crystalline Polymer Actuators. *Adv. Mater.* **2017**, *29*, 1606467.
(41) Lendlein, A.; Jiang, H.; Junger, O.; Langer, R. Light-induced Shape Memory Polymers. *Nature* **2005**, *434*, 879−883.
(42) Zhou, H.; Xue, C.; Weis, P.; Suzuki, Y.; Huang, S.; Koynov, K.; Auernhammer, G. K.; Berger, R.; Butt, H. J.; Wu, S. Photoswitchingof Glass Transition Temperatures of Azobenzene-Containing Polymers Induces Reversible Solid-to-Liquid Transitions. *Nat. Chem.* **2017**, *9*, 145−151.
(43) Xu, W. C.; Sun, S.; Wu, S. Photoinduced Reversible Solid-to-Liquid Transitions Using Photoswitchable Materials. *Angew. Chem., Int. Ed.* **2019**, *58*, 9712−9740.
(44) Zou, W. K.; Dong, J. T.; Luo, Y. W.; Zhao, Q.; Xie, T. Dynamic Covalent Polymer Networks: from Old Chemistryto Modern Day Innovations. *Adv. Mater.* **2017**, *29*, 1606100.
(45) Pei, Z. Q.; Yang, Y.; Chen, Q. M.; Terentjev, E. M.; Wei, Y.; Ji, Y. Mouldable Liquid-Crystalline Elastomer Actuatorswith Exchangeable Covalent Bonds. *Nat. Mater.* **2014**, *13*, 36−41.
(46) Ube, T.; Kawasaki, K.; Ikeda, T. Photomobile Liquid-Crystalline Elastomers with Rearrangeable Networks. *Adv. Mater.* **2016**, *28*, 8212−8217.
(47) Tazuke, S.; Kurihara, S.; Ikeda, T. Amplified Image Recording in Liquid Crystal Media by Means of Photochemically Triggered Phase Transition. *Chem. Lett.* **1987**, *16*, 911−914.
(48) Lin, L.; Yan, Z.; Gu, J. S.; Zhang, Y. Y.; Feng, Z.; Yu, Y. L. UV-Responsive Behavior of Azopyridine-Containing Diblock Copolymeric Vesicles: Photoinduced Fusion, Disintegration and Rearrangement. *Macromol. Rapid Commun.* **2009**, *30*, 1089−1093.

DOI: 10.1021/acsami.9b17271
ACS Appl. Mater. Interfaces 2019, 11, 46212−46218